

The influence of lutetium-doping effect on diffusional creep in polycrystalline Al₂O₃

Hidehiro Yoshida*, Takahisa Yamamoto, Taketo Sakuma

Department of Advanced Materials Science, Graduate School of Frontier Science, The University of Tokyo, 7-3-1 Hongo, Bunkyo-ku, Tokyo, 113-8656 Japan

Received 26 September 2002; received in revised form 17 December 2002; accepted 1 January 2003

Abstract

High temperature compressive creep behavior in high-purity, undoped Al₂O₃ and 0.02 mol% LuO_{1.5}-doped Al₂O₃ with an average grain size of about 5 μm was investigated under an applied stress of 10–100 MPa at 1250–1400 °C. Microstructure and chemical composition at the grain boundaries in the present materials were characterized with a high-resolution transmission electron microscopy (HRTEM) and an energy dispersive X-ray spectroscopy (EDS). The Lu-doping is effective for the improvement in the creep resistance in Al₂O₃ with the grain size of about 5 μm even at the dopant level of 0.02 mol%. Steady-state creep rate in undoped Al₂O₃ is in good agreement with theoretical creep rate of the grain boundary diffusion mechanism. On the other hand, in LuO_{1.5}-doped Al₂O₃, the stress dependence of the creep rate is the same than in undoped one, but the activation energy for the creep deformation is much larger than that in undoped alumina. The large activation energy and the sluggish creep rate in Lu-doped alumina are caused by suppression of grain boundary diffusivity in alumina due to Lu³⁺ cations' segregation. In fact, the effect of 0.02 mol% LuO_{1.5}-doping in Al₂O₃ with the grain size of about 5 μm is very close to that of 0.1 mol% LuO_{1.5}-doping in Al₂O₃ with the grain size of about 1 μm; owing to a similar grain boundary dopant content in the two materials.

© 2003 Elsevier Science Ltd. All rights reserved.

Keywords: Al₂O₃; Creep; Grain boundaries; Small dopant effect; Structural applications

1. Introduction

High temperature creep or plastic flow behavior in polycrystalline Al₂O₃ has been extensively studied, and the high temperature deformation mechanisms under various testing conditions were argued in detail; according to the deformation mechanism map compiled for polycrystalline alumina with a grain size of 10 μm, the high temperature creep deformation often occurs by diffusional flow under a wide range of stresses and temperatures.¹ It has been reported that the predominant deformation mechanism in Al₂O₃ with a grain size of less than 10 μm is grain boundary diffusional creep² at temperatures of 1100–1400 °C and an applied stress of less than 100 MPa,³ and grain boundary sliding becomes important as the grain size is smaller.^{3,4} For

instance, the grain boundary sliding contributes dominantly to high-temperature creep deformation for small grain alumina with the grain size of 1.6 μm at 1673 K under 44 MPa.⁵

One of the striking facts in recent years regarding with the high-temperature plastic deformation in fine-grained Al₂O₃ is a marked effect of a small amount of dopant cation; high-temperature creep resistance in fine-grained, polycrystalline Al₂O₃ with an average grain size of less than 2–3 μm is sensitively affected by a small amount of cation doping. For instance, it was found that the creep rate in polycrystalline Al₂O₃ with a grain size of about 1 μm was reduced by an addition of 0.1 wt.% ZrO₂ by a factor of about 15 at 1250 °C under applied stresses of 10–200 MPa.⁶ It was also revealed that the high-temperature creep rate in Al₂O₃ with the grain size of 1 μm is about 200 times lowered at 1250 °C by doping of lanthanoid oxide such as Y₂O₃ or Lu₂O₃ even in the dopant level of 0.05 mol%.^{7,8} Similar effects of small dopant cation on the high temperature creep resistance in Al₂O₃ have been also reported.^{9–15} More

* Corresponding author. Tel.: +81-3-5841-7154; fax: +81-3-5800-2433.

E-mail address: yoshida@ceramic.mm.t.u-tokyo.ac.jp (H. Yoshida).

recently, it has been revealed with high-resolution transmission electron microscopy (HRTEM) attached with an energy dispersive X-ray spectrometer (EDS) that the small amount of dopant cations segregates at the vicinity of grain boundaries,^{6–8} and the segregated cations are supposed to change chemistry at the grain boundaries in alumina.^{16,17}

Concerning the origin of the dopant effect, there have been a couple of ideas proposed so far,^{11,18} and one explanation is mainly due to the ionic size of the dopant.⁹ However, recent systematic studies for divalent, trivalent and tetravalent cation-doped Al_2O_3 with a grain size of about 1 μm suggested that the reduction in the creep strain rate is not in the same order as increasing the ionic size.^{16,19} This fact means that the dopant effect is not so simple and cannot be considered only by the ionic sizes. In our previous reports,^{16,19} atomic interactions between Al_2O_3 and dopant cations is thus discussed in various kind of cation-doped alumina with a grain size of about 1 μm . The results indicated that ionic bonding strength in alumina with the dopant cations' segregation correlates with difference in the high temperature creep resistance in fine-grained alumina. However, in order to provide evidence that the dopant cations affect the grain boundary diffusivity in Al_2O_3 , and that the small amount of cation doping is effective for the improvement in the creep resistance for wide-ranging condition, it is necessary to examine the dopant effect under the testing conditions for which the dominant rate-controlling mechanism is the grain boundary diffusional creep.

This paper aims to examine an effect of 0.02 mol% $\text{LuO}_{1.5}$ -doping on the high temperature creep resistance in polycrystalline Al_2O_3 with an average grain size of about 5 μm in which the grain boundary diffusional creep tend to be a rate-controlling mechanism at high temperature. In our previous studies, 0.1 mol% $\text{LuO}_{1.5}$ (0.05 mol% Lu_2O_3)-doped Al_2O_3 with the grain size of about 1 μm was used as the specimen, in which the dopant cations tend to distribute uniformly along the grain boundaries.¹⁶ Moreover, Lu^{3+} cation is one of the most effective dopants for the improvement in the high temperature creep resistance.^{8,16} In the present study, one-fifth of the dopant level was chosen; on the assumption that an average width of the grain boundaries where the dopant cations are soluble is independent of the grain size, and that the dopant cations segregate uniformly at the grain boundaries, the concentration of Lu^{3+} cations in 0.02 mol% $\text{LuO}_{1.5}$ -doped Al_2O_3 with the grain size of about 5 μm must be nearly the same with that in 0.1 mol% $\text{LuO}_{1.5}$ -doped Al_2O_3 with the grain size of about 1 μm , because area of the grain boundaries in unit volume is in inverse proportion to the grain size. The dopant effect in the present materials can be argued in comparison with that in fine-grained alumina.

2. Experimental procedures

The present materials used in this study were undoped, high-purity Al_2O_3 and 0.02 mol% $\text{LuO}_{1.5}$ -doped Al_2O_3 . The starting materials were high-purity Al_2O_3 powders (purity > 99.99%, TM-DAR; Taimei Chemistry, Japan) and Lu-acetate (purity > 99.99%, Rare-metallic, Japan). The alumina powders were mixed with the lutetium-acetate solution to yield the doping level, ball-milled in ethanol together with 5mm diameter high-purity alumina balls for 24 h, dried and shifted through a 60 mesh sieve for granulation. The green compacts were prepared by pressing the mixed powders into bars with cemented carbide die under a pressure of 33 MPa, and then isostatically-pressed under a pressure of 100 MPa. The green compacts of undoped- and Lu-doped Al_2O_3 were sintered at 1500 °C for 2 h and 1550 °C for 4 h in air in order to obtain an average grain size of about 5 μm , respectively. The grain size was measured through linear intercept method using photograph obtained by scanning electron microscopy (SEM; JSM-5200, Jeol, Japan). Relative density of the present materials was measured by Archimedes method.

Microstructure in the present materials was examined with transmission electron microscopy (TEM). TEM specimens were prepared using a standard technique involving mechanical grinding to a thickness of 0.1 mm, dimpled to a thickness of 20 μm and ion beam milling to electron transparency at about 4 kV. High-resolution transmission electron microscopy (HRTEM) observations were performed to analyze the grain boundary structure using a Hitachi H-9000NAR (300 kV) transmission electron microscope. Chemical analysis was carried out with an energy dispersive X-ray spectroscopy (EDS; Noran Voyager system) attached to the field-emission type microscope (Topcon-002BF; Topcon, Japan) using a probe size of less than 1 nm, which provide local analysis at the vicinity of grain boundary.

High-temperature creep test was carried out at temperatures in the range of 1250–1400 °C under an applied stress of 10–100 MPa in air by a uniaxial compressive creep testing machine with a resistance-heated furnace (HCT-1000, Toshin Industry, Japan). The size of the creep specimens was 5×5 mm² in cross section and 8 mm in height. The test temperature was measured by a Pt–PtRh thermocouple attached to each specimen and kept to within ±1 °C.

3. Results and discussions

Fig. 1 shows a scanning electron micrograph of an as-sintered (a) undoped, high-purity Al_2O_3 and (b) 0.02 mol% $\text{LuO}_{1.5}$ -doped Al_2O_3 . Fairly uniform and equiaxed grains with an average grain size of about 5

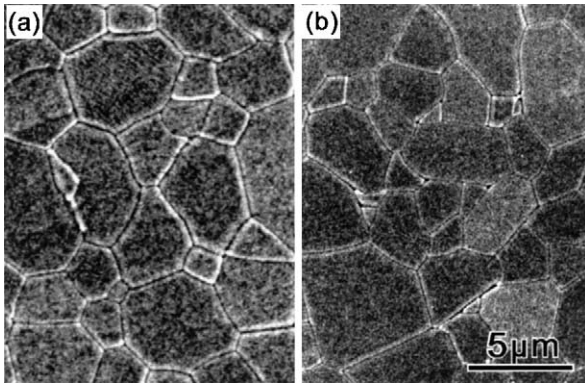


Fig. 1. A scanning electron micrograph of an as-sintered (a) undoped, high-purity Al_2O_3 and (b) 0.02 mol% $\text{LuO}_{1.5}$ -doped Al_2O_3 .

μm were obtained for each material. The average grain size of the present materials is listed in Table 1. The relative density of the present materials is more than 99% of the theoretical density. In $\text{LuO}_{1.5}$ -doped Al_2O_3 , dispersion of second phase particles is not observed both inside grains and at grain boundaries, and the microstructure seems to be a single phase material as well as the undoped- Al_2O_3 .

It was confirmed that 0.02 mol% $\text{LuO}_{1.5}$ -doped Al_2O_3 is essentially single phase material by HRTEM technique. Fig. 2 shows a high-resolution transmission electron micrograph of the grain boundary in 0.02 mol% $\text{LuO}_{1.5}$ -doped Al_2O_3 . Second phase particle or amorphous phase is not found at the grain boundaries, as well as in the 0.1 mol% $\text{LuO}_{1.5}$ (0.05 mol% Lu_2O_3)-doped alumina with the grain size of 0.9 μm .^{16–18} Fig. 3 shows an EDS profile obtained from (a) the grain interior (5 nm off the grain boundary) and (b) the grain boundary in $\text{LuO}_{1.5}$ -doped Al_2O_3 using incident electron beam diameter of 1 nm. Circles in Fig. 2 indicate the analyzed points. As shown in Fig. 3, the presence of lutetium ions is detected only in the grain boundary, and is not detected in the grain interior. The grain boundary segregation of Lu^{3+} cations was also observed in 0.1 mol% $\text{LuO}_{1.5}$ -doped Al_2O_3 with the grain size of 0.9 μm .^{16,17} The present result seems to be reasonable, because the solubility limit of Lu_2O_3 into Al_2O_3 is very low.²⁰

Fig. 4 shows a comparison of creep curves in undoped and $\text{LuO}_{1.5}$ -doped Al_2O_3 under an applied stress of 75 MPa at 1350 °C. The creep deformation in Al_2O_3 is highly suppressed by the doping of 0.02 mol% $\text{LuO}_{1.5}$. The Lu^{3+} -doping is effective to improve the high-temperature creep resistance in Al_2O_3 with the grain size of

about 5 μm even in the dopant level of 0.02 mol%. The improvement in the high temperature creep resistance in 0.02 mol% $\text{LuO}_{1.5}$ -doped Al_2O_3 is not caused by difference in the grain size, because the grain size in the present materials is nearly the same, and grain growth during creep testing was negligible under the testing temperature, which is 100–250 °C lower than the sintering temperature. During the creep deformation, the creep strain rate in the present materials decreases with time, and takes nearly a constant value after about 20 h in undoped Al_2O_3 and about 150 h in Lu-doped Al_2O_3 . In the present study, steady-state creep rate is decided at the testing time when change in the strain rate becomes less than $1 \times 10^{-9} \text{ s}^{-1}$, and is analyzed using the following equation,

$$\dot{\epsilon} = A\sigma^n d^{-p} \exp(-Q/RT) \quad (1)$$

where $\dot{\epsilon}$ is the steady-state creep rate, A is the material constant, σ is the applied stress, d is the grain size, R is the gas constant and T is the testing temperature. The parameters for high temperature creep of n , p , and Q are termed the stress exponent, the grain size exponent and the activation energy for creep deformation, respectively.

On the basis of Eq. (1), Fig. 5 shows a logarithmic plot of the steady-state creep rate against the applied stress in undoped and 0.02 mol% $\text{LuO}_{1.5}$ -doped Al_2O_3 at each temperature examined. The relationship between the creep rate and the applied stress at each temperature exhibits a single straight line for the present materials under the applied stress examined. The creep rate in 0.02 mol% $\text{LuO}_{1.5}$ -doped Al_2O_3 is about 30 times lower than that in undoped one at 1300 °C. The doping of $\text{LuO}_{1.5}$ is very effective for the improvement in the creep resistance in polycrystalline alumina with the grain size of 5 μm as well as for the fine-grained one.^{7,17} The stress exponent is about 1 for the present materials. The stress exponent of 1 is interpreted in terms of either grain boundary diffusional creep² or lattice diffusional creep.^{21,22}

Activation energy for creep deformation can be obtained in a conventional way from an Arrhenius plot of the creep strain rate. Fig. 6 shows the Arrhenius plot of the steady-state creep rate against inverse temperature in undoped Al_2O_3 and 0.02 mol% $\text{LuO}_{1.5}$ -doped Al_2O_3 under the applied stress of 50 MPa. The data in the present materials exhibit single straight lines. From the slope of these lines, the activation energy for undoped and $\text{LuO}_{1.5}$ -doped Al_2O_3 can be estimated to

Table 1
Sintering temperature and obtained average grain size in undoped and 0.02 mol% $\text{LuO}_{1.5}$ -doped Al_2O_3

Sample	Sintering condition	Average grain size (μm)
Undoped Al_2O_3	1500 °C for 2 h	5.4
0.02 mol% $\text{LuO}_{1.5}$ -doped Al_2O_3	1550 °C for 4 h	4.9

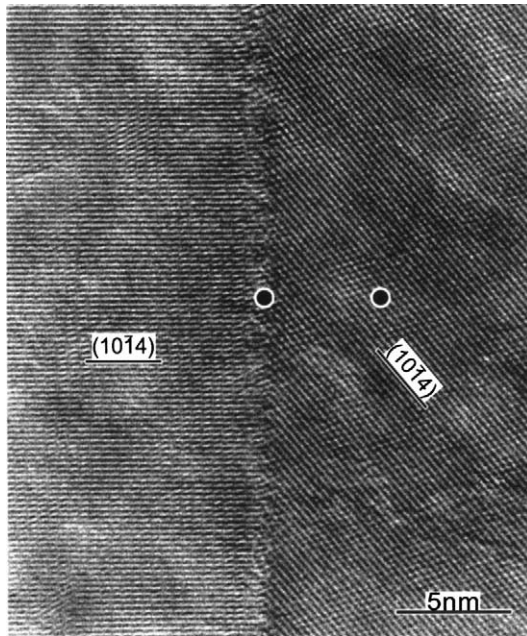


Fig. 2. A high-resolution electron micrograph of a grain boundary in an as-sintered 0.02 mol% $\text{LuO}_{1.5}$ -doped Al_2O_3 . Circles on the grain interior and the grain boundary indicate analyzed area by EDS.

be 410 and 780 kJ/mol, respectively. Since the activation energy for undoped Al_2O_3 is in good agreement with that for Al^{3+} grain boundary diffusion of 418 kJ/mol,²³ and is lower than that for oxygen grain boundary diffusion of 460 kJ/mol²⁴ and that for Al^{3+} or O^{2-} ions'

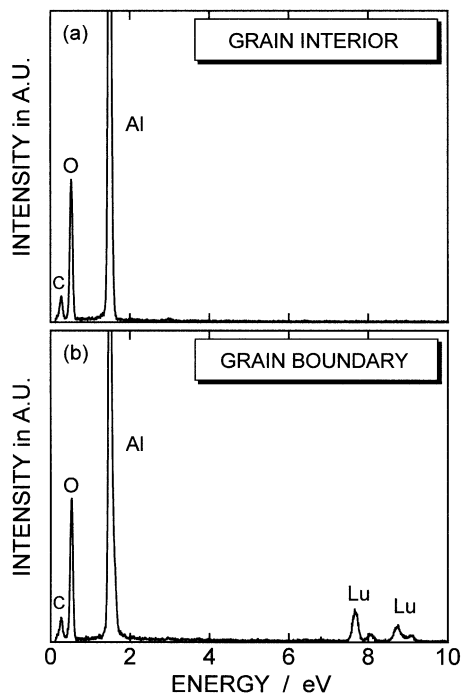


Fig. 3. EDS spectra taken with a probe size of about 1 nm from (a) grain interior (5 nm off grain boundary) and (b) grain boundary in 0.02 mol% $\text{LuO}_{1.5}$ -doped Al_2O_3 . The analyzed area is marked by the circles in Fig. 2.

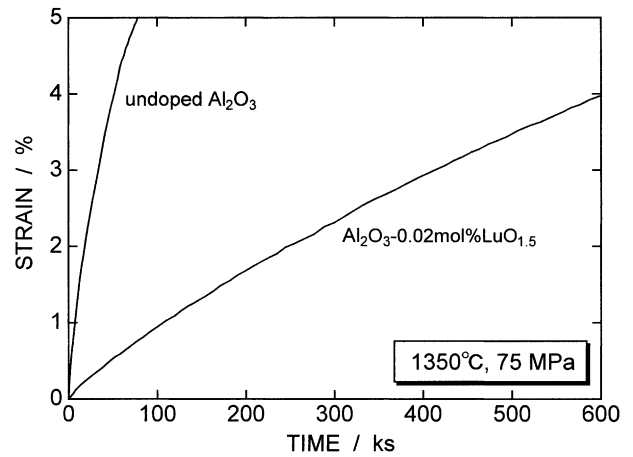


Fig. 4. A comparison of creep curves in undoped and 0.02 mol% $\text{LuO}_{1.5}$ -doped Al_2O_3 under an applied stress of 75 MPa at 1350 °C.

lattice diffusion of 510²⁵ or 636 kJ/mol,²⁶ the creep deformation in undoped- Al_2O_3 is thus supposed to take place by the grain boundary diffusional creep mechanism. On the other hand, the activation energy in $\text{LuO}_{1.5}$ -doped Al_2O_3 is much larger than that in undoped Al_2O_3 , and is even larger than that in the lattice diffusion in Al_2O_3 . However, the large activation energy is supposed not to be associated with sluggish lattice diffusion by Lu^{3+} -doping, based on the following result.

When diffusional mass transport occurs along the grain boundary, the steady-state creep rate is given by

$$\dot{\epsilon} = \frac{148 \delta D_{gb} \Omega \sigma}{\pi kT d^3} \quad (2)$$

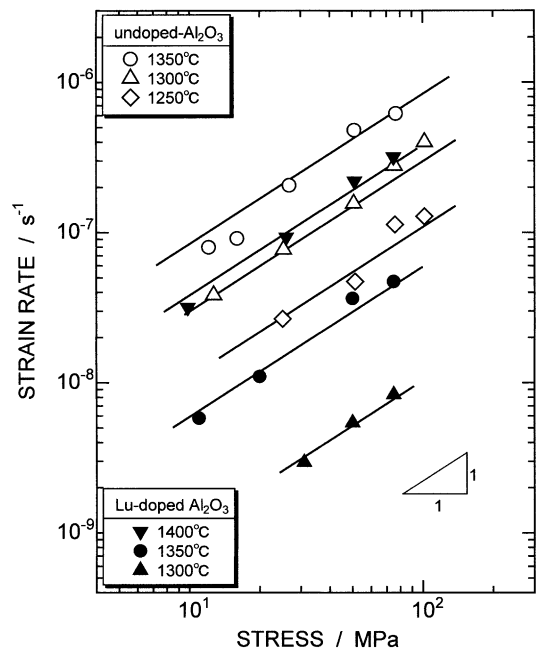


Fig. 5. A logarithmic plot of steady-state creep rate against applied stress in undoped and 0.02 mol% $\text{LuO}_{1.5}$ -doped Al_2O_3 for each testing temperature.

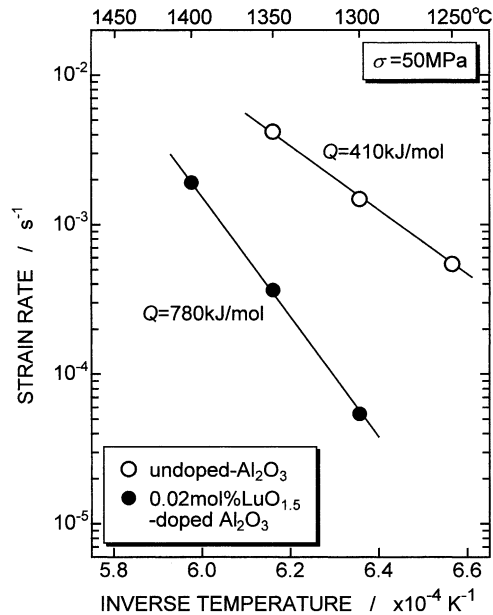


Fig. 6. An Arrhenius plot of steady-state creep rate against inverse temperature in undoped Al_2O_3 and 0.02 mol% $\text{LuO}_{1.5}$ -doped Al_2O_3 . Slope of the lines represents the activation energies for creep deformation.

where δ is the grain boundary width, D_{gb} is the grain boundary diffusivity, Ω is the atomic volume.² Fig. 7 shows a comparison between the experimental creep rate in undoped Al_2O_3 and the theoretical value of the grain boundary diffusional creep. In Fig. 7, broken lines indicate the calculated creep strain rate in undoped Al_2O_3 with the grain size of 5.4 μm using the following expression for δD_{gb} of Al^{3+} cation as $8.6 \times 10^{-10} \exp(-418 \text{ kJ/mol}/RT) \text{ m}^3 \text{ s}^{-1}$,²³ Ω of $\text{AlO}_{1.5}$ as $2.12 \times 10^{-29} \text{ m}^3$ and $d=5.4 \mu\text{m}$.²⁷ As shown in Fig. 7, the experimental creep rate in undoped Al_2O_3 is in good agreement with the calculated creep rate of the grain boundary diffusional creep, while the creep deformation mechanism in fine-grained alumina with the average grain size of 0.9 μm is considered to be grain boundary sliding^{28–31} accommodated by the grain boundary diffusion of Al^{3+} cations.^{6–8,32,33} These results are consistent with the previous reports that the predominant deformation mechanism in alumina with the grain size of less than 10 μm is the grain boundary diffusional creep³ and that the grain boundary sliding contribution to total creep strain becomes major in polycrystalline alumina with a grain size of less than about 2 μm .^{1–5} In other words, the dopant effect for the high temperature creep resistance is caused by the retardation of the grain boundary diffusion in Al_2O_3 due to the Lu^{3+} cations' segregation at the grain boundary.

The value of the activation energy in 0.02 mol% $\text{LuO}_{1.5}$ -doped Al_2O_3 is nearly the same with that in 0.1 mol% $\text{LuO}_{1.5}$ -doped, fine-grained Al_2O_3 with an average grain size of 0.9 μm ; the activation energy in fine-grained Lu -doped Al_2O_3 is estimated to be about 780 kJ/mol.^{7,33} The distribution of the dopant at grain boundaries is similar in the two materials. If the reduction of the steady-state creep rate in fine-grained alumina due to Lu^{3+} -doping results from decrease in the grain boundary diffusivity, the creep strain rate in Lu^{3+} -doped Al_2O_3 with the grain size of 5 μm can be predicted from the difference in the creep strain rate between the fine-grained, undoped and Lu -doped materials.^{7,33} In Fig. 7, gray lines indicate the estimated creep rate in Lu^{3+} -doped Al_2O_3 with the grain size of 4.9 μm . The experimental data in Lu^{3+} -doped alumina is fairly in good agreement with the calculated value. This result indicates that the accommodation process for the creep deformation in fine-grained, Lu -doped Al_2O_3 must be the suppressed grain boundary diffusion, as well as in the present materials. Under the testing conditions that the grain boundary diffusion is the dominant accommodation mechanism, it is expected that the small amount of Lu^{3+} doping is highly effective to improve the high temperature creep resistance in polycrystalline Al_2O_3 .

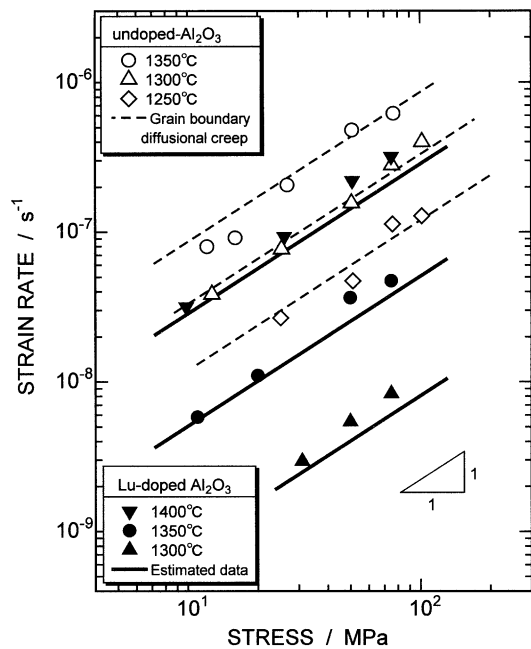


Fig. 7. A comparison between the experimental creep strain rate and theoretical grain boundary diffusional creep rate (broken lines) against the applied stress in high-purity, undoped Al_2O_3 with the average grain size of 5.4 μm . Calculated creep rates for $\text{LuO}_{1.5}$ -doped Al_2O_3 with the grain size of 4.9 μm estimated from the previous data^{7,33} (gray lines) are also plotted, together with the experimental data in 0.02 mol% $\text{LuO}_{1.5}$ -doped Al_2O_3 .

4. Conclusions

High temperature creep behavior in high-purity, undoped polycrystalline Al_2O_3 and 0.02 mol% $\text{LuO}_{1.5}$ -doped Al_2O_3 with an average grain size of about 5 μm was examined under an applied stress of 10–100 MPa at 1250–1400 °C. The creep deformation in Al_2O_3 was highly suppressed by 0.02 mol% $\text{LuO}_{1.5}$ -doping. Steady-state creep rate in undoped Al_2O_3 was in good agreement with theoretical creep rate of grain boundary diffusional creep which was rate-controlled by Al^{3+} cation's grain boundary diffusion. In $\text{LuO}_{1.5}$ -doped Al_2O_3 , dependence of the creep rate on the applied stress was the same as with the undoped one, but activation energy for creep deformation was much larger than that in undoped alumina. Since the creep deformation in Al_2O_3 with the grain size of 5 μm took place mainly by the grain boundary diffusional creep, and since the doped Lu^{3+} cations are segregated at the grain boundaries, it can be concluded that the large activation energy for creep deformation and the sluggish creep rate in 0.02 mol% $\text{LuO}_{1.5}$ -doped Al_2O_3 is attributed to retardation of the grain boundary diffusivity in Al_2O_3 due to the segregation of Lu^{3+} cations. Because area of grain boundaries in unit volume is in inverse proportion to an average grain size, concentration of the dopant cation at the grain boundaries in 0.02 mol% $\text{LuO}_{1.5}$ -doped Al_2O_3 was supposed to be nearly the same than in 0.1 mol% $\text{LuO}_{1.5}$ -doped, fine-grained Al_2O_3 with the grain size of about 1 μm . In fact, the dopant effect was in the same level in both the present material and the fine-grained alumina, nevertheless the total amount of dopant in the present material was one-fifth of that in fine-grained one. The fact must be another evidence that the dopant cations' segregation is the origin of the dopant effect in Lu^{3+} -doped Al_2O_3 . In polycrystalline alumina with the grain size of less than 10 μm , the small amount of Lu^{3+} doping is expected to be highly effective for creep resistance.

Acknowledgements

We wish to express gratitude to the Ministry of Education, Science and Culture, Japan for the financial support by a Grant-in-Aid for Scientific Research (A) (2)-13305052 and Grant-in-Aid for Young Scientists (B)-13750647. The authors thank Dr. K. Okada for assistance with experimental work.

References

1. Frost, H. J. and Ashby, M. F., *Deformation-Mechanism Maps*. Pergamon, Oxford, 1982, p. 98.
2. Coble, R. L., A model for boundary diffusion controlled creep in polycrystalline materials. *J. Appl. Phys.*, 1979, **34**, 1679–1682.
3. Heuer, A. H., Cannon, R. M. and Tighe, N. J., Plastic deformation of fine-grained alumina. In *Ultrafine-Grain Ceramics*, ed. J. J. Burke, N. L. Reed and V. Weiss. Syracuse University Press, Syracuse, NY, 1970, pp. 339–365.
4. Heuer, A. H., Tighe, N. J. and Cannon, R. M., Plastic deformation of fine grained alumina: II, basal slip and nonaccommodated grain-boundary sliding. *J. Am. Ceram. Soc.*, 1980, **63**, 53–58.
5. Chokshi, A. H., An evaluation of the grain-boundary sliding contribution to creep deformation in polycrystalline alumina. *J. Mater. Sci.*, 1990, **25**, 3221–3228.
6. Yoshida, H., Okada, K., Ikuhara, Y. and Sakuma, T., Improvement of high-temperature creep resistance in fine-grained Al_2O_3 by Zr^{4+} segregation in grain boundaries. *Philos. Mag. Lett.*, 1997, **76**, 9–14.
7. Yoshida, H., Ikuhara, Y. and Sakuma, T., High-temperature creep resistance in rare earth-doped fine-grained Al_2O_3 . *J. Mater. Res.*, 1998, **13**, 2597–2601.
8. Yoshida, H., Ikuhara, Y. and Sakuma, T., High-temperature creep resistance in lanthanoid ion-doped polycrystalline Al_2O_3 . *Philos. Mag. Lett.*, 1999, **79**, 249–256.
9. Cho, J., Harmer, M. P., Chan, H. M., Rickman, J. M. and Thompson, A. M., Effect of yttrium and lanthanum on the tensile creep behavior of aluminum oxide. *J. Am. Ceram. Soc.*, 1997, **80**, 1013–1017.
10. Lartigue, S., Priester, L., Dupau, F., Gruffel, P. and Carry, C., Dislocation activity and differences between tensile and compressive creep of yttria-doped alumina. *Mater. Sci. Eng.*, 1993, **A164**, 211–215.
11. Cho, J., Wang, C. M., Chan, H. M., Rickman, J. M. and Harmer, M. P., *Acta Mater.*, 1999, **47**, 4197–4207.
12. Wang, C., Cargill, G. S., Chan, H. M. and Harmer, M. P., Structural features of Y-saturated and supersaturated grain boundaries in alumina. *Acta Mater.*, 2002, **48**, 2579–2591.
13. Lartigue-Korinek, S., Carry, C. and Priester, L., Multiscale aspects of the influence of yttrium on microstructure, sintering and creep of alumina. *J. Eur. Ceram. Soc.*, 2002, **22**, 1525–1541.
14. Gulgun, M. A., Voytovich, R., Maclaren, I., Ruhle, M. and Cannon, R. M., Cation segregation in an oxide ceramic with low solubility: Yttrium doped alpha-alumina. *Interface Sci.*, 2002, **10**, 99–110.
15. Yoshida, H., Takigawa, Y., Ikuhara, Y. and Sakuma, T., Effect of chemical bonding state on high-temperature plastic flow behavior in fine-grained, polycrystalline cation-doped Al_2O_3 . *Mater. Trans.*, 2002, **43**, 1566–1572.
16. Yoshida, H., Ikuhara, Y. and Sakuma, T., Grain boundary electronic structure related to the high-temperature creep resistance in polycrystalline Al_2O_3 . *Acta Mater.*, 2002, **50**, 2955–2966.
17. Yoshida, H., Ikuhara, Y. and Sakuma, T., Improvement of creep resistance in polycrystalline Al_2O_3 by Lu-doping. *J. Inorganic Materials*, 1999, **1**, 229–234.
18. Swiatnicki, W., Lartigue-Korinek, S. and Laval, J. Y., Grain boundary structure and intergranular segregation in Al_2O_3 . *Acta Metal. Mater.*, 1995, **43**, 795–805.
19. Yoshida, H., Yamamoto, T., Ikuhara, Y. and Sakuma, T., A change in the chemical bonding strength and high-temperature creep resistance in Al_2O_3 with lanthanoid oxide doping. *Philos. Mag. A*, 2002, **82**, 511–525.
20. Wu, P. and Pelton, A. D., Coupled thermodynamic-phase diagram assessment of the rare earth oxide-aluminum oxide binary systems. *J. Alloys Compounds*, 1992, **179**, 259–287.
21. Nabarro, F.R.N., Deformation of crystals by the motion of single ions. In *Rep. Conf. Strength of Solids*. 1947. The Physical Society, London, 1948, pp. 75–90.
22. Herring, C., Diffusional viscosity of a polycrystalline solid. *J. Appl. Phys.*, 1950, **21**, 437–445.
23. Cannon, R. M., Rhodes, W. H. and Heuer, A. H., Plastic deformation of fine-grained alumina (Al_2O_3): I, interface-controlled diffusional creep. *J. Am. Ceram. Soc.*, 1980, **63**, 46–53.

24. Oishi, Y. and Kingery, W. D., Self-diffusion of oxygen in single crystal and polycrystalline aluminum oxide. *J. Chem. Phys.*, 1960, **33**, 480–486.
25. Gall, M. L., Lesage, B. and Bernardini, J., Self-diffusion in α -Al₂O₃ I. Aluminium diffusion in single crystals. *Philos. Mag. A*, 1994, **70**, 761–773.
26. Prot, D. and Monty, C., Self-diffusion in α -Al₂O₃ II. Oxygen diffusion in 'undoped' single crystals. *Philos. Mag. A*, 1996, **73**, 899–917.
27. Lee, W. E. and Lagerlof, K. P. D., Structural and electron diffraction data for sapphire (α -Al₂O₃). *J. Electron Microscopy Technol.*, 1985, **2**, 247–258.
28. Gifkins, R. C., Grain-boundary sliding and its accommodation during creep and superplasticity. *Metall. Trans. A*, 1976, **7**, 1225–1232.
29. Langdon, T. G., Grain boundary sliding as a deformation mechanism during creep. *Philos. Mag.*, 1970, **22**, 689–700.
30. Mukherjee, A. K., The rate controlling mechanism in superplasticity. *Mater. Sci. Eng.*, 1971, **8**, 83–89.
31. Arieli, A. and Mukherjee, A. K., A model for the rate-controlling mechanism in superplasticity. *Mater. Sci. Eng.*, 1980, **45**, 61–70.
32. Yoshida, H. and Sakuma, T., Transient creep associated with the grain boundary sliding in fine-grained, single-phase Al₂O₃. *J. Mater. Sci.*, 1998, **33**, 4879–4885.
33. Yoshida, H., Ikuhara, Y. and Sakuma, T., Transient creep in fine-grained polycrystalline Al₂O₃ with Lu³⁺ ion segregation at the grain boundaries. *J. Mater. Res.*, 2001, **16**, 716–720.